Optimization of Type-II AlAs/AlInAs/GaAsSb Heterostructure at 1550 nm Under Well-Width Variation

Priya, Chaudhary
Department of Electronics and Communication Engineering, Manipal University Jaipur

Rathi, Amit
Department of Electronics and Communication Engineering, Manipal University Jaipur

Amit Kumar Singh
Department of Electronics and Communication Engineering, Manipal University Jaipur

Md. Riyaj
Department of Electronics and Communication Engineering, Vidya Vihar Institute of Technology

https://doi.org/10.5109/7236839

出版情報：Evergreen. 11 (3), pp.1882-1891, 2024-09. 九州大学グリーンテクノロジー研究教育センター
バージョン：

Optimization of Type-II AlAs/AlInAs/GaAsSb Heterostructure at 1550 nm Under Well-Width Variation

Priya Chaudhary[1], Amit Rathi[1,*], Amit Kumar Singh[1], Md. Riyaj[2]
[1]Department of Electronics and Communication Engineering, Manipal University Jaipur, Jaipur, Rajasthan, India
[2]Department of Electronics and Communication Engineering, Vidya Vihar Institute of Technology, Purnea, Bihar, India

*Author to whom correspondence should be addressed:
E-mail: pch4332@gmail.com; amitrathi1978@gmail.com

(Received May 6, 2024; Revised August 14, 2024; Accepted August 30, 2024).

Abstract: A W-shaped type-II AlAs/$Al_{0.3}In_{0.7}As$ /$GaAs_{0.1}Sb_{0.9}$ lasing nanoscale heterostructure is designed for near infrared emission. The Luttinger kohn 6*6 model is used to compute wavefunctions, dispersion, matrix elements and then optical gain. The calculated optical gain for x polarization of light is found under variable well widths. For injected carrier concentration of 2.5×10^{12} /cm^2, gain of 12560/cm is attained at a wavelength of 1550 nm for 2 nm quantum well width. Such a structure can be regarded as new because of its high optical gain with low attenuation at 1550 nm, which makes it useful for optoelectronics.

Keywords: AlAs; AlInAs; GaAsSb; type-II QW heterostructure; dispersion; optical gain; near-infrared region.

1. Introduction

During the last decade, the type-II quantum well heterostructures based on III-V semiconductors have been the subject of extensive research for applications in the infrared spectrum[1)]. To develop tunable hetero junction devices, III-V semiconductor materials are considered to be useful materials[2,3)]. For optoelectronics, Jain et al.[4)] surveyed III-V group elements and heterostructures. Optronic device performance has dramatically improved due to the invention of nanoscale heterostructures, novel materials and their properties, and increased production capabilities[5)]. Researchers have found type-II heterostructures to be particularly appealing, and type-II band alignment heterostructure are currently in use to build opto-devices like detectors, LEDs, and lasers[6)]. Since the transition between optical bands takes place at a longer wavelength than in type-I heterostructure, these structures effectively used to create laser diodes that can operate in near infrared, mid infrared, far infrared regions[7)]. Nitride based nano heterostructure InGaAsN/GaAs with attractive wavelength of 1.30 µm in infrared region is highly valued in fibre optic communication[8)]. Heterostructures based on III-nitride are widely used to create incredibly powerful infrared lasers[9)]. To design a particular application-based type-I and type-II heterostructures, process flow diagram is depicted in Fig. 1. After applying Hamiltonian model and self-consistent calculation, sub-band dispersion and envelope wavefunction calculation performed. Hence, to achieve high optical gain, analyse dipole transition and movement matrix element then optimize optical gain. Optical gain can check at different parameters such as variable temperature, variable well width, external electric field, uniaxial strain etc.

Recently, InGaAs/GaAsSb type-II heterostructure designed by Nirmal et al.[10)] and achieved the gain of 9000 /cm (1.95 µm) in short wave infrared region. Pan et al. designed and modelled type-II InAlAs/InGaAs/GaAsSb heterostructure at InP substrate for mid infrared laser applications[11)]. Khan et al. presented InAlAs/InGaAs/ GaAsSb type-II heterostructure for 2nm quantum well width and obtained high gain of 6000/cm at 1.55 µm wavelength (0.80eV) in NIR region[12)]. Optical gain for InGaAs/InGaAlAs QW heterostructure is presented for thin quantum well width of 3.2 nm and achieved gain of 11/cm in near infrared (1550 nm) region by Novikov et al.[13)]. The type-I AlGaAs/GaAsP heterostructure is investigated under various electric field and find applications in the range of 708 nm to 826 nm (NIR region) by Singh et al.[14)]. Comprehending the optical properties of semiconductor optronic devices is crucial. The Sb element based heterostructures for infrared region under different conditions like variable well width, under electric field and uniaxial strain, variable temperature etc. have been discussed in detail by Chaudhary et al.[15)]. The band gap tailoring is crucial to design semiconductor nanoscale heterostructures in optronic devices[16)]. In QW heterostructures, photon amplification take place when carriers recombine radiatively in optical area[17)]. Berger et

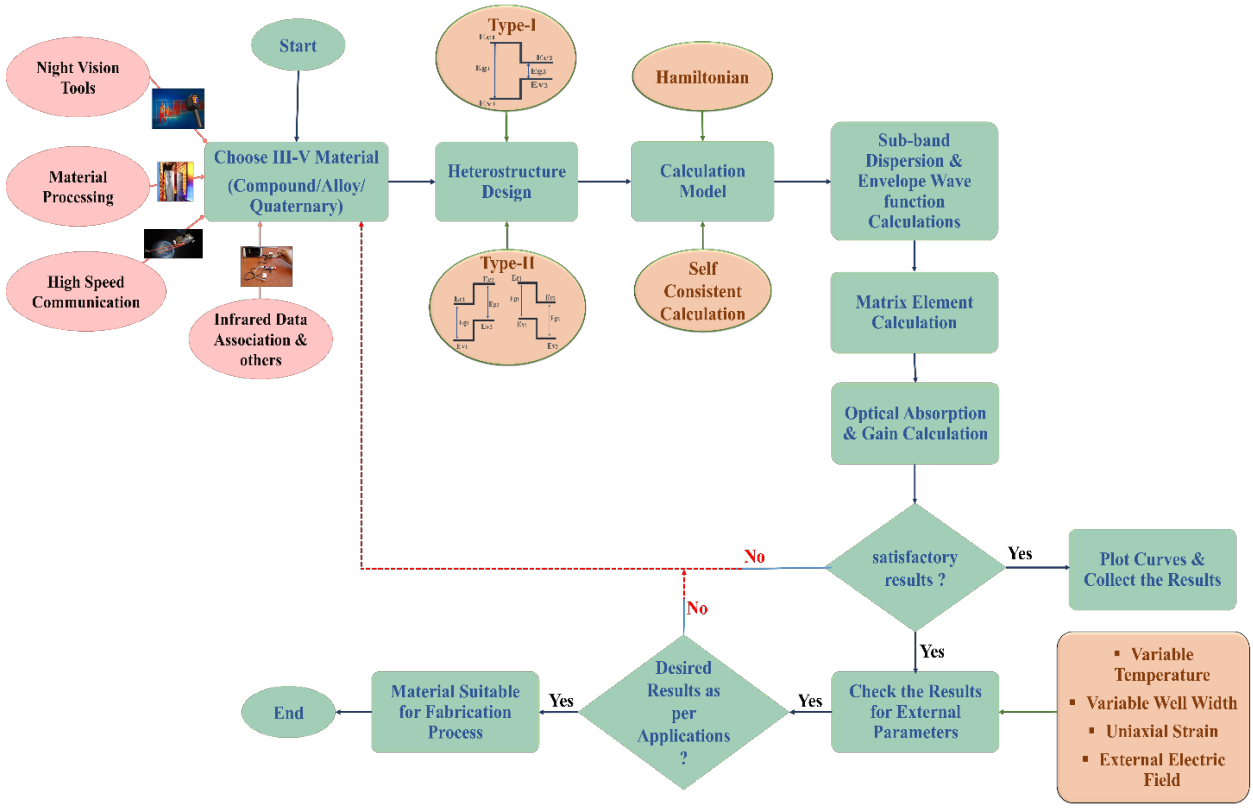

Fig. 1: Process flow diagram

al. designed type-II W-shaped QW heterostructure for lasing applications in near infrared region[18,44].

Nano scale InGaAs/GaAsSb/InAlAs heterostructure is also devoted to near infrared regime and 6070 /cm gain is achieved using k.p method at 100 K temperature[19]. The type-II InGaAs/GaAsSb/InAlAs heterostructure grown on GaAs substrate and find appropriate for 1650 nm wavelength[20]. Babichev et al. presented InGaAlAs/InGaAs/InP heterostructure for 1520-80 nm radiation wavelength[21]. Enhanced intermixing[22] or interdiffusion[23,45] approach is required to attain tunability[24] and better device performance[25]. The InAlAs/InGaAs (intermixing) heterostructure is designed and obtained gain for 6 nm well width and gain peak is achieved for near infrared lasing (1.47 µm) wavelength[26]. The GaAsSb material-based type-II heterostructure are designed to provide better tunability or lattice matching and offer strong carrier mobility. Haider et al. presented a GaAsSb based type-II with an optical gain of 8850/cm for $1.5\times10^{12}/cm^2$ charge density and found applications in the mid-infrared (5200 nm) range, like mid-infrared spectroscopy, industrial, and telecommunication[27]. A W-shaped type-II heterostructure is created using a GaAsSb layer of 2 nm and an InAlAs layer of 10nm width that produce high gain in near-infrared (1550 nm) range[28]. In GaAsSb/InGaAs heterostructure, the GaAsSb layer is employed as a barrier (2 nm thickness) and altered wavelength found between 1550 nm and 1650 nm for different (5GPa-20GPa) uniaxial pressure[29]. Garima et al. designed a type-II M-shaped InGaAs/InAs/GaAsSb heterostructure under uniaxial strain for mid infrared applications[30]. Electron mobility is studied in InAlAs/InP heterostructure at room temperature by Aina et al.[31]. The type-II InAlAs/AlSb heterostructure is designed to produce optical gain in near infrared regime and achieve 1662/cm for $5\times10^{12}/cm^2$ charge density[32].

This study presents a novel W-shaped type-II nanoscale heterostructure (AlAs/AlInAs/GaAsSb) developed on InP substrate, with simulation results under various well widths that are found to be acceptable for NIR applications. The optical gain is calculated for 2nm, 3nm. 4nm and 5nm quantum well width. The substrate InP is preferred over GaAs substrate, because of low cost, superior morphology of the surface, and better thermal conductivity. The type-II nanoscale heterostructure is created because of its longer wavelength and higher intensity and cover the region of infrared. Experimental/theoretical data for the AlAs/AlInAs/GaAsSb heterostructure design is not available for variable well widths. A high optical gain is obtained for near-infrared lasing applications using this heterostructure. The proposed heterostructure design employs the same sandwich quantum well GaAsSb layer, as in previous research work. Whereas, in order to attain the desired high optical gain and strong interband transition, alternative AlInAs quantum well layers and AlAs barrier layers are employed. The theory and design of the heterostructure ($AlAs/Al_{0.3}In_{0.7}As/GaAs_{0.1}Sb_{0.9}$) are covered in the following part, after which the conclusion is presented.

2. Heterostructure design details

The bulk energy band structure for $Al_{0.3}In_{0.7}As$/InP and $GaAs_{0.1}Sb_{0.9}$/InP developed on the substrate InP (300K) to determine the kind of strain resulting from the lattice mismatch, shown in Fig. 2. In both materials, the lattice matched condition, or the absence of strain, is indicated by the heavy hole band (HHB-red colour) that is above the light hole band (LHB-green colour) and overlap. Figure 2 exhibits the bandgaps of $Al_{0.3}In_{0.7}As$ and $GaAs_{0.1}Sb_{0.9}$, which are 1.001 eV and 0.667 eV, respectively. Vegard's low[33] yields an accurate lattice constant of 5.939 Å for $Al_{0.3}In_{0.7}As$ and 6.051 Å for $GaAs_{0.1}Sb_{0.9}$ alloys. Consequently, the lattice matches for $f_{Al0.3In0.7As}$ and $f_{GaAs0.1Sb0.9}$ are 1.20% and 3.12%, respectively. In Fig. 2(a) and 2(b), the conduction band is quasi-parabolic for both $Al_{0.3}In_{0.7}As$/InP and $GaAs_{0.1}Sb_{0.9}$/InP bulk material and valence sub band (heavy hole band) is not parabolic for both bulk materials.

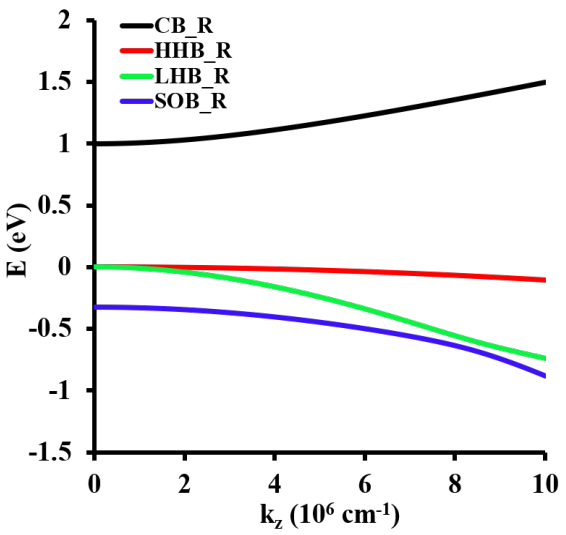

(a)

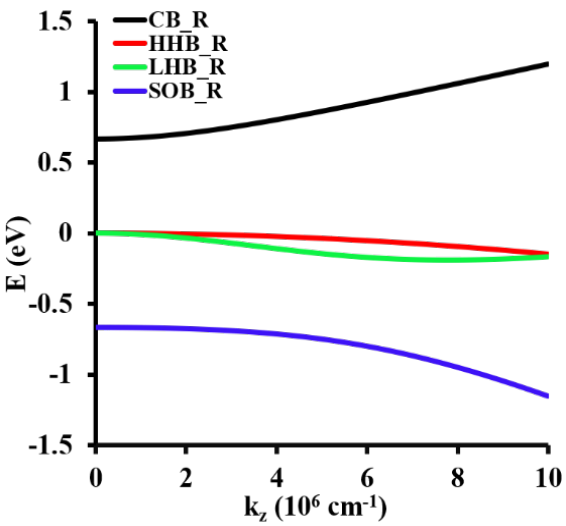

(b)

Fig. 2: Bulk band structures (a) $Al_{0.3}In_{0.7}As$ /InP and (b) $GaAs_{0.1}Sb_{0.9}$/InP.

In proposed novel heterostructure, quantum well is made up of two p-type AlInAs layers of 2 nm each and one n-type GaAsSb layer together, that is sandwiched between them. The AlAs layers are used as barrier. InP substrate is used to create the entire substrate. Optical gain is computed under different well width. Thus, four distinct quantum-well widths (GaAsSb layer) of 2 nm, 3 nm, 4 nm, and 5nm are taken into consideration. As the well width increases, the overall size of heterostructure varies from 120 to 150nm. The three sub bands that make up the valence band in the band structure are heavy hole band (HHB-red colour), light hole band (LHB-green colour), and split off band (SOB-sky blue colour).

Since the conduction band and split off energy band are relatively far apart, light emission cannot be effectively inferred from it. In addition, the band arrangement is type-II, meaning that optical and electrical transition occur between holes confined in GaAsSb layer (valence band) and electrons confined in AlInAs layers (conduction band)[34]. The conduction band 6×6 Kohn-Luttinger model is employed to compute the band structure, sub band dispersion and associated wavefunctions. The 6×6 Hamiltonian matrix is reformed into 3×3 block diagonalised matrix form to minimize the size of system as stated in equation (1).

$$H_{6\times6}(k) = \begin{pmatrix} H^{+}_{3\times3} & 0 \\ 0 & H^{-}_{3\times3} \end{pmatrix} \tag{1}$$

where, the terms $H^{+}_{3\times3}$ and $H^{-}_{3\times3}$ are as follows [37]:

$$H^{U}_{3\times3} = -\begin{pmatrix} P+Q-V_h(Z) & R(k)\pm iS(k) & \sqrt{2}R(k)\pm\frac{i}{\sqrt{2}}S(k) \\ R(k)\pm iS(k) & P-Q-V_h(z) & \sqrt{2}Q\pm i\sqrt{\frac{3}{2}}S(k) \\ \sqrt{2}R(k)\pm\frac{i}{\sqrt{2}}S(k) & \sqrt{2}R(k)\mp\sqrt{\frac{3}{2}}S(k) & P+\Delta_{so}-V_h(Z) \end{pmatrix} \tag{2}$$

where Δ_{so}, and V_h are split-off energy and unstrained valence band edge, respectively. Here, P=P(k)+P(ε), Q=Q(k)+Q(ε) are expanded in equations (3) and (4). The terms S(k) and R(k) are also described below in equations (5), (6) [38].

$$P(k) = \left(\frac{\hbar^2}{2m}\right)\gamma_1 k_t^2 + k_z^2 \quad \text{and,}$$

$$P(\varepsilon) = -a_v(\varepsilon_{xx}+\varepsilon_{yy}+\varepsilon_{zz}) \tag{3}$$

$$Q(k) = \left(\frac{\hbar^2}{2m}\right)\gamma_2(k_t^2 - 2k_z^2) \quad \text{and,}$$

$$Q(\varepsilon) = -\frac{b}{2}\left(\varepsilon_{xx}+\varepsilon_{yy}-2\varepsilon_{zz}\right) \tag{4}$$

$$S(k) = \left(\frac{\hbar^2}{2m}\right)\sqrt{3}\left(\frac{\gamma_2+\gamma_3}{2}\right)k_t^2 \tag{5}$$

$$R(k) = \left(\frac{\hbar^2}{2m}\right) 2\sqrt{3}\gamma_3 k_t k_z \quad (6)$$

In above equations, k_t^2 is the addition of k_x^2 and k_y^2, and Luttinger parameters are γ_1, γ_2 and, γ_3. The parameters a_v and b denotes the Bir-Pikus deformation potential.

3. Simulation results and discussion

The major goal is to identify a high optical gain for infrared radiation emission. The Fermi Golden rule is applied to determine the optical gain by first determining its wavefunction, charge carriers (electrons/holes) and associated energy levels[35]. For wavefunction calculation, the k.p Hamiltonian 6×6 diagonalized matrix is derived and Luttinger-Kohn model[36] is used in this structure. Injected carrier concentration is 2.5×10^{12} /cm^2 and equilibrium (electron and hole) concentrations are 4×10^{12} /cm^2. In this type-II AlAs/$Al_{0.3}In_{0.7}As$/$GaAs_{0.1}Sb_{0.9}$ nanoscale heterostructure, Figure 3 displays the estimated electron and hole wavefunctions for various quantum well widths (2, 3, 4 and 5nm).

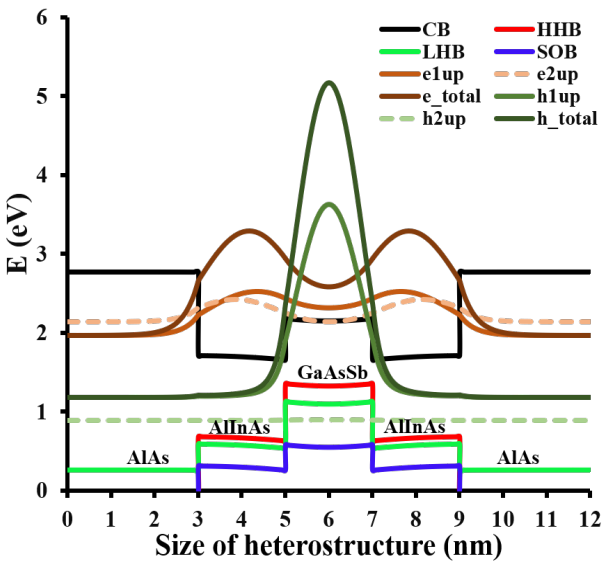

(a) Wavefunction for 2 nm well width

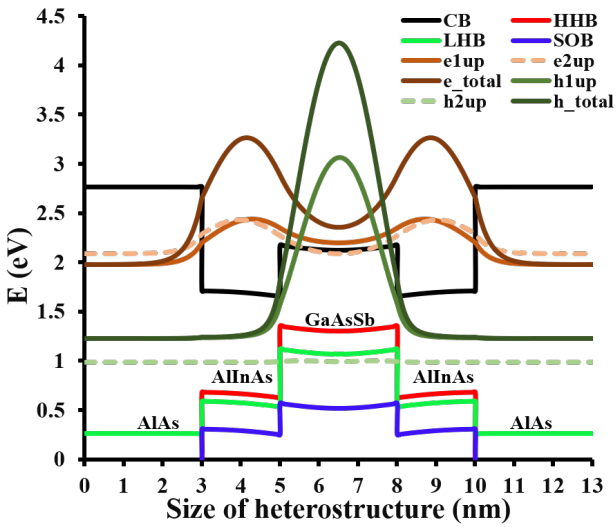

(b) Wavefunction for 2 nm well width

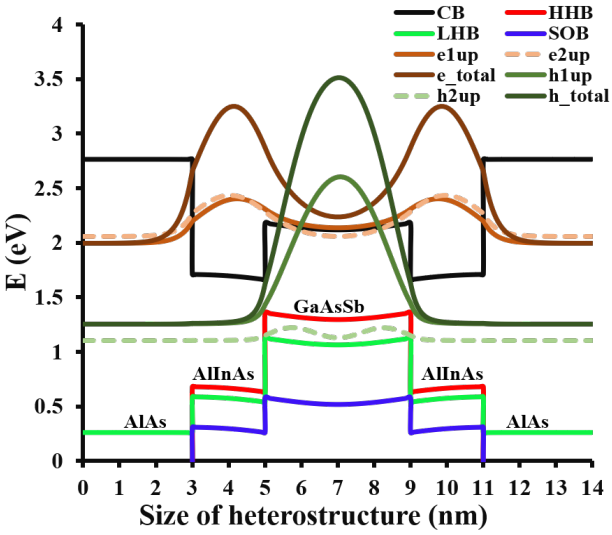

(c) Wavefunction for 4 nm well width

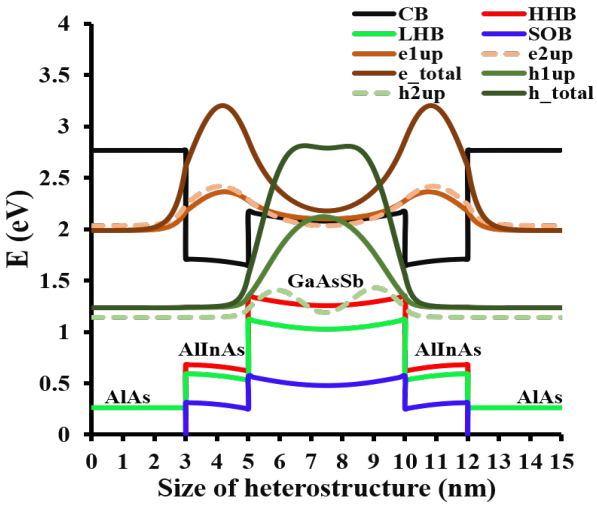

(d) Wavefunction for 4 nm well width

Fig. 3: Energy band diagrams with total wave function in AlAs/ AlInAs/GaAsSb heterostructure under well width variation.

The first and second energy level electron wavefunctions (e1-up, e2-up) are confined in conduction band and first energy level hole (h1-up, h2-up) in valence band well region. The total hole density in the GaAsSb region (highlighted in dark green) and the total electron density in the two AlInAs regions (highlighted in dark brown) are attained in each figure of wavefunction for each quantum well width. It can be inferred from this Fig. 3 that the total hole density is higher $GaAs_{0.1}Sb_{0.9}$ layer of valence band and total electron density is higher in $Al_{0.3}In_{0.7}As$ layers of conduction band. Here, as the quantum well width rises from 2nm to 5nm, a drop in the overall hole and electron density is observed. As a result, higher optical gain is achieved from optical transitions between electrons and holes. In order to create a nano scale heterostructure, certain parameters must be calculated, including the envelope wavefunction, sub band dispersion, and matrix elements (dipole and momentum) between the energy levels.

After wavefunction computation, the sub band dispersion profiles for increasing well widths are calculated for proposed AlAs/AlInAs/GaAsSb heterostructure at 300K and curves are displayed in Fig. 4. Figure 4(a), (b), (c), and (d) demonstrate that as quantum well width increases, the dispersed electronic states (es_1, es_2 and es_3) exhibit a shift from semi-parabolic to parabolic. Conversely, non-parabolic states exist for dispersed holes (hs_1, hs_2 and hs_3). The electronic state es_3 is located further away from state es_1, but electronic energy states es_1and es_2 approach one another as well width increase. In the same manner, the energy states of hole hs_2 and hs_3 is relatively near to one another, although the initial hole state hs_1 is located at distance from hs_2 energy state. As well width increase, energy hole states hs_1 and hs_2 approach one another. Energy is almost same at k_r=0 point for all electronic and hole states as well width increase. The probable transitions for the optical gain take place from es_1 and es_2 to hs_1 and hs_2.

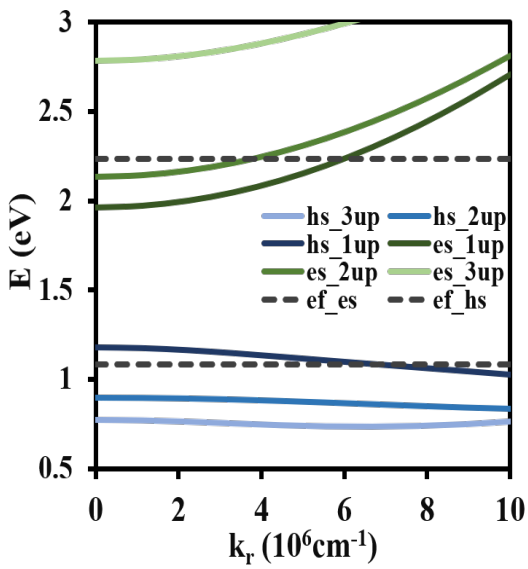

(a) Dispersion profile for 2 nm QW

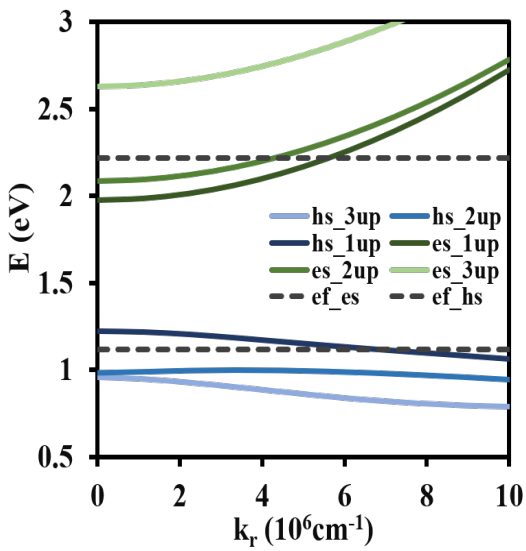

(b) Dispersion profile for 3 nm QW

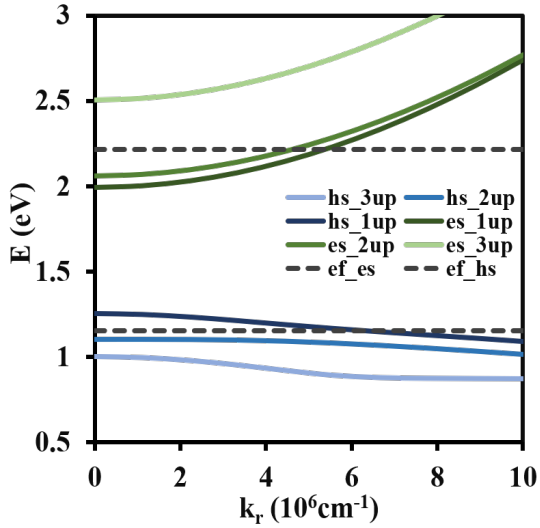

(c) Dispersion profile for 4 nm QW

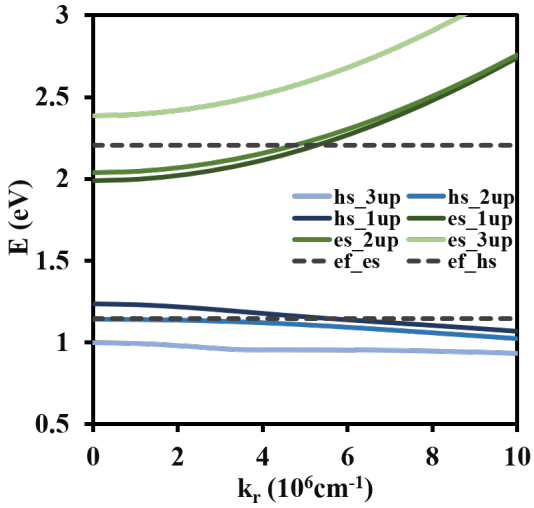

(e) Dispersion profile for 5 nm QW

Fig. 4: Dispersion profile of AlAs/AlInAs/GaAsSb heterostructure for variable well widths (2, 3, 4, and 5 nm).

The dipole and momentum matrix elements depicted for different well widths (2, 3, 4, and 5nm) in Fig. 5 and Fig. 6, respectively, crucial to analyse because they represent the transition strength between the energy levels where electrons and holes are inhibited, which create transitions and causes optical gain. Figure 5 indicate that the properties of the gain at k_r (wave vector) =0 that are affected by the x-group of transition e1-h1 mainly but z-group of transition e1-h2 shows maximum contribution (at k_r=0) to the optical gain for 2 nm well width. There is no contribution at k_r=0 from z-group of transition e1-h1 to the gain, however, the contribution rises with increasing k_r values and cross over. For higher value of k_r, inter sub-band transition e1-h1 of x-group drop gradually. At k_r=0, the contribution of x-groupe1-h2 and z-groupe1-h2 transition is almost zero to the gain characteristics except 2 nm dipole transition as shown in Fig. 5 (a). However, with rising values of k_r, the x-groupe1-h2 and z-groupe1-h2 transition tend to decrease slightly.

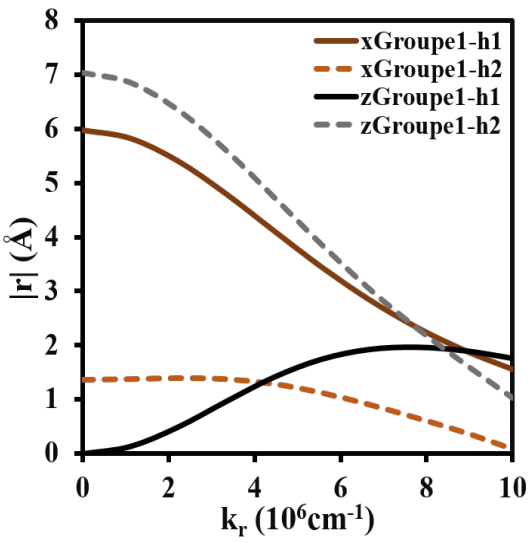

(a) Dipole transition for 2 nm QW

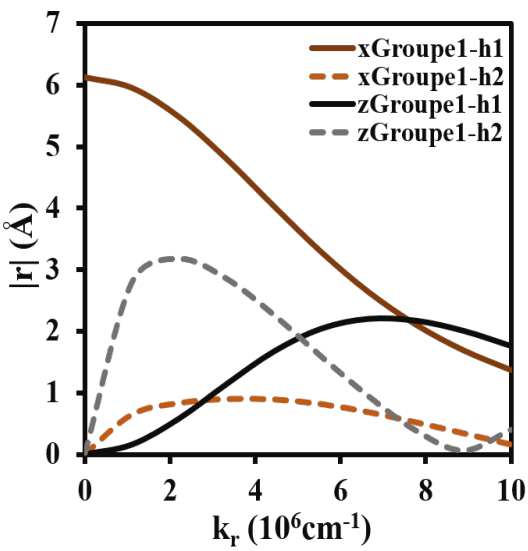

(b) Dipole transition for 3 nm QW

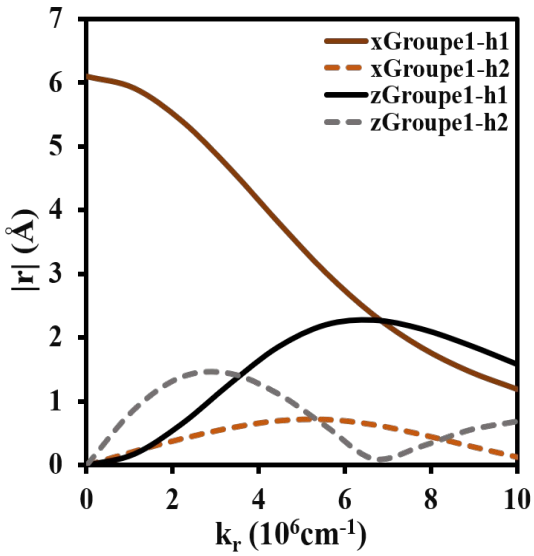

(c) Dipole transition for 4 nm QW

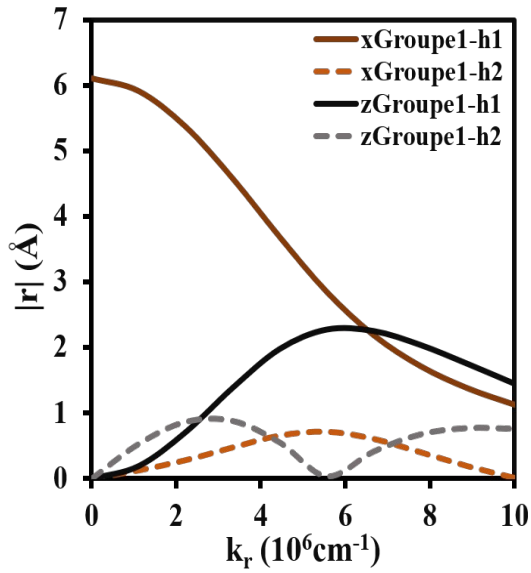

(d) Dipole transition for 5 nm QW

Fig. 5: Dipole matrix elements transitions for AlAs/ AlInAs/GaAsSb type-II heterostructure for variable well widths in x and z polarization.

Consequently, at some higher value of k_r, a contribution is seen in the gain characteristics for proposed different well widths dipole transition. Figure 6 presents the squared momentum matrix elements transitions for x group and z group transition between e1-h1 and e1-h2 for different well widths of proposed nano scale hetero-structure. The inter sub-band transition of x-group e1-h1 for squared momentum matrix elements indicates the gain contribution at wave vector k_r=0, while z-group e1-h1 has no contribution at zero value of k_r. With increasing quantum well widths, the contribution of matrix elements transition of x-groupe1-h1 decreases gradually at k_r=0. On the other hand, for increasing value of k_r, the squared momentum matrix elements transition of x-groupe1-h2 has no contribution to optical gain. The transition of z-

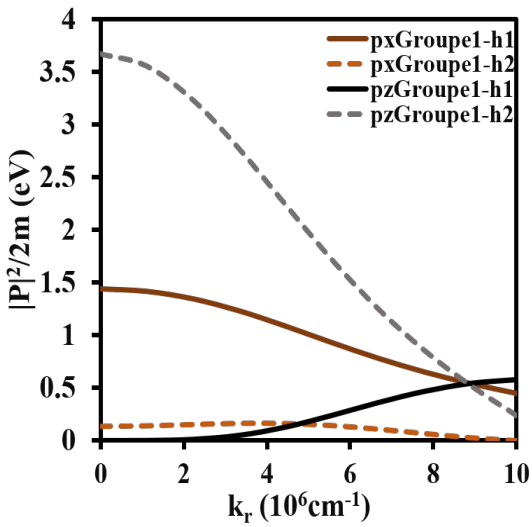

(a) Momentum matrix element for 2 nm QW

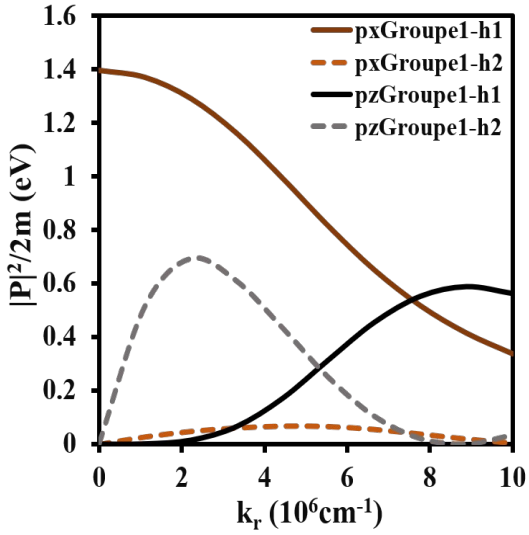

(b) Momentum matrix element for 3 nm QW

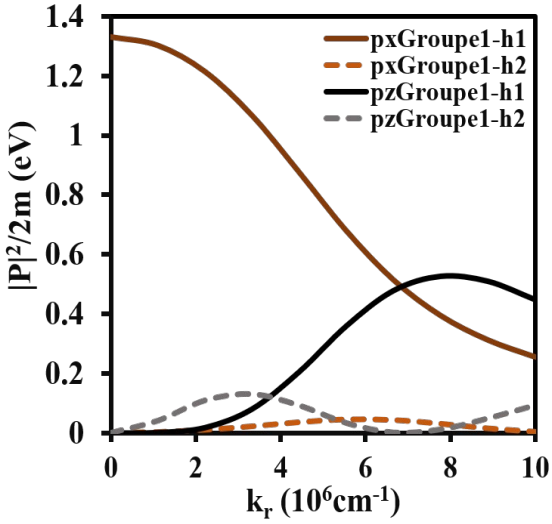

(c) Momentum matrix element for 4 nm QW

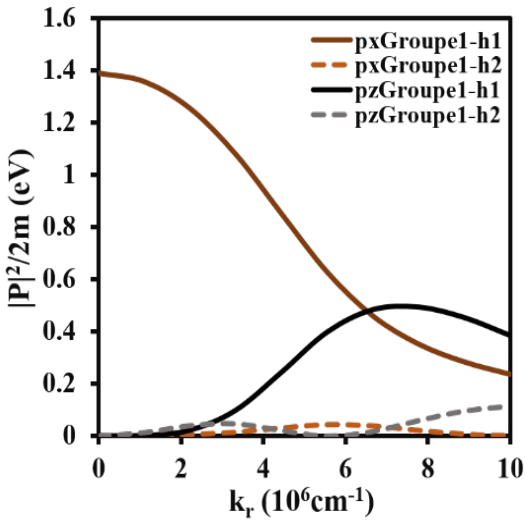

(d) Momentum matrix element for 5 nm QW

Fig. 6: Momentum matrix elements for different well widths in x and z polarization.

groupe1-h2 shows the maximum contribution (at k_r=0) to the gain for 2 nm well width but for increasing value of k_r, this contribution continuously decreases as well width increases. The optical gain of presented nano sale heterostructure is determined by computing the matrix elements. The optical gain (x polarization) with different well widths (2, 3, 4, and 5nm) at 300K is displayed in Fig.7. The performance of this heterostructure is also compared with other designed type-II heterostructures and overall evaluation of gain under various well width, and wavelength, that are indicated in Table 1.

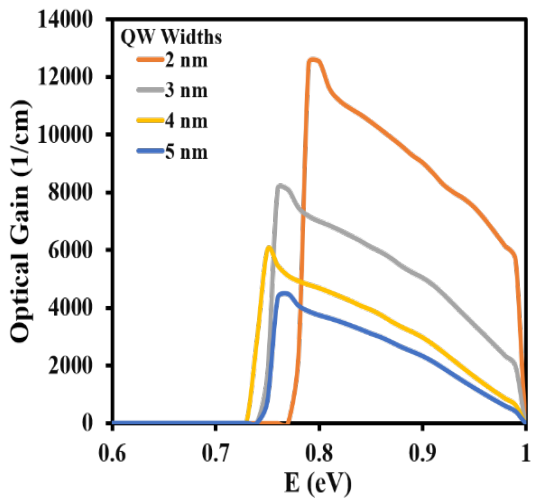

Fig. 7: Optical gain of AlAs/$Al_{0.3}In_{0.7}As$/ $GaAs_{0.1}Sb_{0.9}$ nanoscale heterostructure in x polarization under various well width variations.

Table 1. Comparison of $AlAs/Al_{0.3}In_{0.7}As/GaAs_{0.1}Sb_{0.9}$ type-II heterostructures with other heterostructures in the terms of optical gain under different well width and wavelengths.

S. No.	Different QW nanoscale heterostructures	Type	Quantum Well Widths (nm)	Gain (/cm)	λ (μm)	Ref.
1.	$In_{0.52}Al_{0.48}As/GaAs_{0.51}Sb_{0.49}$ $/In_{0.53}Ga_{0.47}As$	II	5	1600	1.98	11)
2.	InGaAs/GaAsSb	II	2	6220	1.55	34)
3.	$In_{0.45}Ga_{0.55}As/GaAs_{0.31}Sb_{0.69}$	II	6	1000	2.6	39)
4.	$In_{0.5}Ga_{0.5}As_{0.8}P_{0.2}/GaAs_{0.5}Sb_{0.5}$	II	2	8000	1.85	40)
5.	$In_{0.25}Ga_{0.75}As/InAs/GaAs_{0.31}Sb_{0.69}$	II	2	4800	3.2	41)
6.	InAlAs/InGaAs/GaAsSb	II	4	6000	1.55	42)
7.	InAlAs/InGaAs/GaAsSb	II	2 3	5931 2647	1.42 1.90	43)
8.	$AlAs/Al_{0.3}In_{0.7}As/GaAs_{0.1}Sb_{0.9}$ (W-shaped, InP substrate)	II	2 3 4 5	12560 (0.80 eV) 8144 (0.76 eV) 6008 (0.75 eV) 4486 (0.77 eV)	1.550 1.631 1.653 1.610	Present work

Under x polarization, the higher optical gain of $AlAs/Al_{0.3}In_{0.7}As/GaAs_{0.1}Sb_{0.9}$ nanoscale heterostructure is 12560/cm at 1550 nm for a 2 nm well width. The increasing well widths 3nm, 4nm, and 5nm, the optical gain of 8144/cm, 6008/cm and 4486/cm achieved, respectively. The designed nano heterostructure find gain spectrum in near infrared range i.e. 1550nm to 1610nm. The result confirms that the developed heterostructure can be employed for fibre optic applications because of its low attenuation at 1550 nm wavelength. For increasing well widths, corresponding wavelength also increases. A left shift and a progressive decline are seen in the optical gain.

4. Conclusion

In this article, a high optical gain is reported for 'W-shaped' type-II $AlAs/Al_{0.3}In_{0.7}As/GaAs_{0.1}Sb_{0.9}$ nanoscale heterostructure. Firstly, the bulk band structure, wavefunctions related to valence band and conduction bands, sub band dispersion, matrix elements (dipole and momentum) are computed and lastly, optical gain is determined under variable quantum well width. The 6×6 kohn Luttinger model is used for computation. Carrier concentration for equilibrium electrons and holes is considered 4×10^{12} cm^{-2} and for injected electrons and holes is 2.5×10^{12} cm^{-2}. It appears that proposed heterostructure operates in the energy range of 0.80 eV to 0.75 eV.

Peak optical gain shifts upwards as the quantum well width decreases from 5 nm to 2 nm, resulting in a drop in emission wavelength. It is evident from the results that the $AlAs/Al_{0.3}In_{0.7}As/GaAs_{0.1}Sb_{0.9}$ heterostructure's optical gain may be effectively utilised for near infrared (NIR) range (1.5 μm - 1.6 μm) applications such as night vision tools, inspection, range finders, surveillance, telecommunication, imaging, material processing etc.

Acknowledgements

Authors would like to thank the Department of Electronics and Communication Engineering, Manipal University Jaipur for providing the simulation facilities at the Electronics and Simulation Lab. Authors are obliged to Dr. Konstantin Kolokolov - Faculty of Physics, M. V. Lomonosov Moscow State University, Russia) for his support with the Heterostructure Design Studio software.

References

1) S.G. Anjum, N. Yadav, H.K. Nirmal, M. Sharma, M.J. Siddiqui, and P.A. Alvi, "Investigation of optical response in type-ii inas/alsb nano-scale heterostructure: a novel dual structure," *Mater. Today Proc.*, **5** (*1*) 1691–1695 (2018). doi:10.1016/j.matpr.2017.11.265.
2) P. Chaudhary, A. Rathi, and A.K. Singh, "First-principles calculation of structural, electronic, and optical properties of $InP_{1-x}Sb_x$ using wc-mbj for nanoscale IR applications," *Nanosci. Technol. An Int. J.*, (2023). doi:10.1615/NANOSCITECHNOLINTJ.2023050162.
3) P. Chaudhary, A. Rathi, and A.K. Singh, "Opto-electronic properties of $GaP_{1-x}Sb_x$ alloys for ir applications," *Crystal Research and Technology,* 2300346 (2024). doi.org/10.1002/crat.202300346
4) J. Jain, A. Rathi, and P. Chaudhary, "III & v group elements and heterostructures for optoelectronics: a survey," *Lect. Notes Electr. Eng.*, **1065** 293–303 (2024). doi:10.1007/978-981-99-4795-9_28/COVER.
5) A.K. Singh, M. Riyaj, S.G. Anjum, N. Yadav, A. Rathi, M.J. Siddiqui, and P.A. Alvi, "Anisotropy and optical gain improvement in type-ii in0.3ga0.7as/gaas0.4sb0.6 nano-scale heterostructure under external uniaxial strain," *Superlattices Microstruct.*, **98** 406–415 (2016).

doi:10.1016/j.spmi.2016.08.048.

6) P. Chaudhary, S. Gour, and A. Rathi, "Survey of Nanosensors and Nano-heterostructures," in: 2022: pp. 67–75. doi:10.1007/978-981-16-6482-3_7.
7) W.W. Bewley, C.L. Felix, E.H. Aifer, I. Vurgaftman, L.J. Olafsen, J.R. Meyer, H. Lee, R.U. Martinelli, J.C. Connolly, A.R. Sugg, G.H. Olsen, M.J. Yang, B.R. Bennett, and B. V. Shanabrook, "Above-room-temperature optically pumped midinfrared w lasers," *Appl. Phys. Lett.*, **73** (*26*) 3833–3835 (1998). doi:10.1063/1.122909.
8) K. Sandhya, G. Bhardwaj, R. Dolia, P. Lal, S. Kumar, S. Dalela, F. Rahman, and P.A. Alvi, "Optimization of optical characteristics of in 0.29 ga 0.71 as 0.99 n 0.01 /gaas straddled nano-heterostructure," *Opto-Electronics Rev.*, **26** 210–216 (2018). doi:10.1016/j.opelre.2018.06.003.
9) P. Chaudhary, A.K. Singh, and A. Rathi, "Recent research in optical characteristics of nitride based nanoscale heterostructures for uv applications," *Lect. Notes Electr. Eng.*, **892** 273–281 (2023). doi:10.1007/978-981-19-1645-8_27/COVER.
10) H.K. Nirmal, N. Yadav, F. Rahman, and P.A. Alvi, "Optimization of high optical gain in type-ii in0.70ga0.30as/gaas0.40sb0.60 lasing nano-heterostructure for swir applications," *Superlattices Microstruct.*, **88** 154–160 (2015). doi:10.1016/j.spmi.2015.09.006.
11) C.H. Pan, and C.P. Lee, "Design and modeling of inp-based ingaas/gaassb type-ii 'w' type quantum wells for mid-infrared laser applications," *J. Appl. Phys.*, **113** (*4*) (2013). doi:10.1063/1.4789634.
12) A.M. Khan, G. Bhardwaj, M. Abu-Samak, S.H. Saeed, and P.A. Alvi, "Simulating 1.55 µm Optical Gain in Type-II InAlAs/InGaAs/GaAsSb Nanoscale Heterostructure," in: IOP Conf. Ser. Mater. Sci. Eng., Institute of Physics Publishing, 2019. doi:10.1088/1757-899X/594/1/012003.
13) I.I. Novikov, L.Y. Karachinsky, E.S. Kolodeznyi, V.E. Bougrov, A.S. Kurochkin, A.G. Gladyshev, A. V. Babichev, I.M. Gadzhiev, M.S. Buyalo, Y.M. Zadiranov, A.A. Usikova, Y.M. Shernyakov, A. V. Savelyev, I.A. Nyapshaev, and A.Y. Egorov, "On the gain properties of 'thin' elastically strained ingaas/ingaalas quantum wells emitting in the near-infrared spectral region near 1550 nm," *Semiconductors*, **50** (*10*) 1412–1415 (2016). doi:10.1134/S1063782616100201.
14) A.K. Singh, A. Rathi, M. Riyaj, K. Sandhya, G. Bhardwaj, and P.A. Alvi, "Wavefunctions and optical gain in al0.8ga0.2as/gaas0.8p0.2 type-i qw-heterostructure under external electric field," *2017 Int. Conf. Comput. Commun. Electron. COMPTELIX 2017*, 59–62 (2017). doi:10.1109/COMPTELIX.2017.8003938.
15) P. Chaudhary, and A. Rathi, "Nanoscal heterostructure concept and III-Sb element based heterostructures for infrared applications: a review," *Nanosci. Technol. An Int. J.*, **15** (*1*) 11–26 (2024). doi:10.1615/NANOSCITECHNOLINTJ.2023045593.
16) Y.A. Aleshchenko, V. V. Kapaev, Y. V. Kopaev, P.S. Kop'ev, V.M. Ustinov, and A.E. Zhukov, "BEHAVIOR of electron states in gaas/algaas double quantum well structure with strongly asymmetric barriers in an external electric field," *Https://Doi.Org/10.1142/S0219581X04001997*, **3** (*1–2*) 203–211 (2011). doi:10.1142/S0219581X04001997.
17) A. David, and B. Miller, "Optical physics of quantum wells," in: Quantum Dyn. Simple Syst., CRC Press, 2020: pp. 239–266. doi:10.1201/9781003072973-9.
18) C. Berger, C. Möller, P. Hens, C. Fuchs, W. Stolz, S.W. Koch, A. Ruiz Perez, J. Hader, and J. V. Moloney, "Novel type-ii material system for laser applications in the near-infrared regime," *AIP Adv.*, **5** (*4*) 47105 (2015). doi:10.1063/1.4917180/595790.
19) M.I. Khan, P.M.Z. Hasan, E.Y. Danish, M. Aslam, S. Kattayat, S. Kumar, S. Dalela, M.A. Ahmad, and P.A. Alvi, "Fine tunability of optical gain characteristics of ingaas/gaassb/inalas nano-heterostructure under combined effect of field and temperature," *Superlattices Microstruct.*, **156** (2021). doi:10.1016/j.spmi.2021.106982.
20) M.I. Khan, G. Bhardwaj, S. Kattayat, S. Sharma, and P.A. Alvi, "Impact of temperature on optical properties of ingaas/gaassb/inalas nano-scale heterostructure," *AIP Conf. Proc.*, **2369** (*1*) (2021). doi:10.1063/5.0061072/669102.
21) A. V Babichev, A.S. Kurochkin, E.S. Kolodeznyi, A.G. Gladyshev, I.I. Novikov, L.Y. Karachinsky, and A.Y. Egorov, "MOLECULAR BEAM EPITAXY GROWN STRAINED HETEROSTRUCTURES FOR ACTIVE REGION OF LASER DIODE WITH EMISSION WAVELENGTH 1520-1580 NM," 2015.
22) J.H. Marsh, "Quantum well intermixing," *Semicond. Sci. Technol.*, **8** (*6*) 1136 (1993). doi:10.1088/0268-1242/8/6/022.
23) I. Harrison, "Impurity-induced disordering in iii-v multi-quantum wells and superlattices," *J. Mater. Sci. Mater. Electron.*, **4** (*1*) 1–28 (1993). doi:10.1007/BF00226629/METRICS.
24) S. Bürkner, S. Weisser, J. Rosenzweig, R.E. Sah, J. Fleissner, J.D. Ralston, and E.C. Larkins, "Wavelength tuning of high-speed ingaasgaas-aigaas pseudomorphic mqw lasers via impurity-free interdiffusion," *IEEE Photonics Technol. Lett.*, **7** (*9*) 941–943 (1995). doi:10.1109/68.414662.
25) W.C.H. Choy, and E.H. Li, "The applications of an interdiffused quantum well in a normally on electroabsorptive fabry-perot reflection modulator," *IEEE J. Quantum Electron.*, **33** (*3*) 382–392 (1997). doi:10.1109/3.556007.
26) M.C.Y. Chan, Y. Chan, and E. Herbert Li, "Modeling

of Optical Gain Properties of Multiple Cations InGaAs-InAlAs Quantum-Well Intermixing," 1998.

27) Haider, Syed Firoz, Upendra Kumar, Sandhya Kattayat, Smitha Josey, M. Ayaz Ahmad, Saral K. Gupta, Rakesh Sharma, Mohammed Ezzeldien, and P. A. Alvi. "Investigation of high optical gain (MIR region) in AlSb/InAs/GaAsSb type-II quantum well heterostructure." *Results in Optics* 5 (2021): 100138.
28) Khan, M. Imran, A. M. Khan, Sandhya Kattayat, Garima Bhardwaj, Savaş Kaya, Saurabh Dalela, Shalendra Kumar, and P. A. Alvi. "Uniaxial ultra-high pressure dependent tuning of optical gain of W-shaped Type-II GaAsSb/InGaAs/InAlAs nano-heterostructure." *Optik* 204 (2020): 164121.
29) Khan, A. M., Sandhya Kattayat, Sandeep Sharma, S. H. Saeed, and P. A. Alvi. "Tuning of gain spectra in GaAsSb/InGaAs heterostructure." In *AIP Conference Proceedings*, vol. 2220, no. 1. AIP Publishing, 2020.
30) Bhardwaj, Garima, Nisha Yadav, S. G. Anjum, M. J. Siddiqui, and P. A. Alvi. "Uniaxial strain induced optical properties of complex type-II InGaAs/InAs/GaAsSb nano-scale heterostructure." *Optik* 146 (2017): 8-16.
31) Aina, Leye, and Mike Mattingly. "Electron mobilities of AlInAs and AlInAs/InP heterostructures." *Journal of applied physics* 64, no. 10 (1988): 5253-5255.
32) Singh, Amit Kumar, Rohit Singh, Dibyendu Chowdhury, and Amit Rathi. "Optical Response in Strained Type-II AlInAs/AlSb Ultrathin QW Heterostructure." In *Flexible Electronics for Electric Vehicles: Select Proceedings of FlexEV—2021*, pp. 569-575. Singapore: Springer Nature Singapore, (2022).
33) Jacob, K. T., Shubhra Raj, and L. Rannesh. "Vegard's law: a fundamental relation or an approximation?." *International Journal of Materials Research* 98, no. 9: 776-779 (2007).
34) J. Vijay, R. krishan Yadav, P.A. Alvi, A. K. Singh, and A. Rathi, "Design and modeling of ingaas/gaassb nanoscale heterostructure for application of optical fiber communication system," *Mater. Today Proc.*, **30** (*xxxx*) 128–131 (2020). doi:10.1016/j.matpr.2020.05.097.
35) A.K. Singh, A. Rathi, M. Riyaj, G. Bhardwaj, and P.A. Alvi, "Optical gain tuning within ir region in type-ii in0.5ga0.5as0.8p0.2/gaas0.5sb0.5 nano-scale heterostructure under external uniaxial strain," *Superlattices Microstruct.*, **111** 591–602 (2017). doi:10.1016/j.spmi.2017.07.014.
36) D. Sytnyk, and R. Melnik, "The luttinger-kohn theory for multiband hamiltonians: a revision of ellipticity requirements," (2018). http://arxiv.org/abs/1808.06988.
37) Harrison, Paul, and Alex Valavanis, "Quantum wells, wires and dots: theoretical and computational physics of semiconductor nanostructures," *John Wiley & Sons*, (2016).
38) Shun, L. C., "Physics of optoelectronics devices," *John Wiley & Sons,* (1995).
39) B. Chen, W. Y. Jiang, and A. L. Holmes, "Design of strain compensated InGaAs/GaAsSb type-II quantum well structures for mid-infrared photodiodes," *Optical and Quantum Electronics*, **44** 103-109 (2012). doi.org/10.1007/s11082-011-9524-1.
40) R. Dolia, G. Bhardwaj, A. K. Singh, S. Kumar, and P. A. Alvi, "Optimization of Type-II 'W'shaped InGaAsP/GaAsSb nanoscale-heterostructure under electric field and temperature," *Superlattices and Microstructures*, **112** 507-516 (2017). doi.org/10.1016/j.spmi.2017.10.007.
41) N. Yadav, G. Bhardwaj, S.G. Anjum, S. Dalela, M.J. Siddiqui, P.A. Alvi, "Investigation of high optical gain in complex type-II InGaAs/InAs/GaAsSb nano-scale heterostructure for MIR applications," *Appl. Opt.*, **56** (No. 15) (2017).
42) A.M. Khan, M. Sharma, M.I. Khan, S. Kattayat, G. Bhardwaj, M. Abu-Samak, S. H. Saeed, and P. A. Alvi, "Optical gain characteristics of a novel InAlAs/InGaAs/GaAsSb type-II nano-heterostructure," *Optik*, **183** 842-848 (2019).
43) Md. Riyaj, A. Rathi, A. K. Singh, Pushpalata, and P.A. Alvi, "Bandgap tailoring and optical response of InAlAs/InGaAs/GaAsSb double quantum well heterostructures: the impact of uniaxial strain and well width variations," *Journal of Modern Optics,* **69** no. 21, 1229-1238 (2022).
44) Sharma, Nishant, Devesh Chandra, Amit Rathi, and A. K. Singh. "First-principles WC-GGA and mBJ calculations for structural, electronic, optical and elastic properties of MxGa1-xSb (M= Al, In, B) ternary alloys." *Materials Science in Semiconductor Processing* 151 (2022): 107033.
45) Riyaj, Md, Amit Rathi, Pushpalata Pushpalata, Sujeet Kumar, Jitendra Kumar, and P. A. Alvi. "Investigation of high optical gain in type-I AlSb/InGaAsSb/AlSb nano-scale heterostructure for NIR applications." In *AIP Conference Proceedings*, vol. 2494, no. 1. AIP Publishing, 2022.